

# Relationship between crystal structure and multiferroic orders in orthorhombic perovskite manganites

## - Supplemental Materials -

Natalya S. Fedorova,<sup>1,\*</sup> Yoav William Windsor,<sup>2</sup> Christoph Findler,<sup>1</sup> Mahesh Ramakrishnan,<sup>2</sup> Amadé Bortis,<sup>3</sup> Laurenz Rettig,<sup>2</sup> Kenta Shimamoto,<sup>4</sup> Elisabeth M. Bothschafter,<sup>2</sup> Michael Porer,<sup>2</sup> Vincent Esposito,<sup>2</sup> Yi Hu,<sup>4</sup> Aurora Alberca,<sup>2</sup> Thomas Lippert,<sup>4,5</sup> Christof W. Schneider,<sup>4</sup> Urs Staub,<sup>2</sup> and Nicola A. Spaldin<sup>1,†</sup>

<sup>1</sup> Materials Theory, ETH Zürich, Wolfgang-Pauli-Strasse 27, CH-8093 Zürich, Switzerland

<sup>2</sup> Swiss Light Source, Paul Scherrer Institut, CH-5232 Villigen PSI, Switzerland

<sup>3</sup> Laboratory for Multifunctional Ferroic Materials, ETH Zürich,  
Vladimir-Prelog-Weg 4, CH-8093 Zürich, Switzerland

<sup>4</sup> Laboratory for Multiscale Materials Experiments,  
Paul Scherrer Institut, CH-5232 Villigen PSI, Switzerland

<sup>5</sup> Laboratory of Inorganic Chemistry, Department of Chemistry and  
Applied Biosciences, ETH Zürich, CH-8093, Zürich, Switzerland

## I. CRYSTAL STRUCTURES

Table I present a list of all crystalline films indicated in the experimental section (Sec. III of the main text). The last entries are values taken from literature. Error estimates of  $q_b$  values are smaller than the last digit. All substrates were YAlO<sub>3</sub> unless otherwise indicated. The incommensurate modulation  $q_b$  varies with temperature.  $q_b$  values here are given at the experimental base temperature of 10 K.

In Table II we summarize experimentally reported (Refs. 5–10) and theoretically optimized lattice parameters of bulk o-RMnO<sub>3</sub> ( $R$ =Gd, Tb, Ho, Er, Yb, Lu), which were discussed in Sec. V of the main text. Table III shows the experimentally measured (Refs. 3 and 4 and our measurements) and theoretically optimized lattice parameters of the corresponding strained films (see Sec. V of the main text). We provide .cif files for all theoretically optimized structures in Supplemental materials.

Table I. Experimentally acquired parameters of epitaxial o-RMnO<sub>3</sub> films. Thickness ( $t$ ) and substrate normal ( $n$ ) are controlled growth parameters.  $q_b$  is deduced from RXD experiments at the Mn  $L$  edges. Error estimates of  $q_b$  values are smaller than the last digit (unless otherwise indicated). Lattice constants were deduced in conventional XRD experiments.

$R$	$t$ (nm)	$n$	$q_b$	$a$ (Å)	$b$ (Å)	$c$ (Å)	Comment
Yb	400	[010]	0.4747	$5.223 \pm 0.004$	$5.771 \pm 0.007$	$7.361 \pm 0.008$	
Er	400	[010]	0.4496	$5.235 \pm 0.002$	$5.799 \pm 0.002$	$7.359 \pm 0.002$	
Er	30	[010]	0.5015	$5.1735 \pm 0.0005$	$5.828 \pm 0.001$	$7.360 \pm 0.001$	
Ho	240	[010]	$0.4007 \pm 0.0001$	$5.275 \pm 0.001$	$5.789 \pm 0.005$	$7.392 \pm 0.001$	Grown on NdGaO <sub>3</sub>
Ho	120	[010]	$0.4138 \pm 0.0002$	$5.2748 \pm 0.0007$	$5.779 \pm 0.005$	$5.420 \pm 0.004$	Grown on NdGaO <sub>3</sub>
Tm	400	[010]	0.4625	$5.235 \pm 0.001$	$5.779 \pm 0.001$	$7.3737 \pm 0.0008$	Windsor <i>et al.</i> <sup>1</sup>
Tm	56	[110]	$0.4704 \pm 0.0001$	$5.221 \pm 0.001$	$5.757 \pm 0.004$	$7.342 \pm 0.005$	
Lu	104	[010]	0.4861	$5.2200 \pm 0.0001$	$5.753 \pm 0.005$	$7.3797 \pm 0.0008$	
Lu	400	[110]	0.4956	$5.191 \pm 0.002$	$5.760 \pm 0.004$	$7.365 \pm 0.004$	
Lu	90	[110]	$0.4933 \pm 0.0001$	$5.175 \pm 0.002$	$5.717 \pm 0.001$	$7.370 \pm 0.002$	
Lu	78	[010]	0.4857	$5.230 \pm 0.005$	$5.766 \pm 0.005$	$7.380 \pm 0.007$	
Lu	26	[010]	0.4797	$5.220 \pm 0.005$	$5.734 \pm 0.005$	$7.492 \pm 0.007$	
Tb	10	[010]	$0.4539 \pm 0.0001$	$5.259 \pm 0.001$	$5.801 \pm 0.001$	$7.355 \pm 0.001$	
Tb	200	[010]	$0.2619 \pm 0.0001$	/	$5.8014 \pm 0.0001$	/	
Y	40	[010]	0.491	??	??	??	Wadati <i>et al.</i> <sup>2</sup>
Tb	14	[010]	0.5	5.182	5.936	7.367	Shimamoto <i>et al.</i> <sup>3</sup>
Gd	10	[010]	0.5	5.183	5.976	7.372	Shimamoto <i>et al.</i> <sup>4</sup>

Table II. Experimentally reported (Exp.) and theoretically optimized (PS) lattice parameters of bulk o- $RMnO_3$ .  $a$ ,  $b$  and  $c$  are the lattice constants of  $Pbnm$  (#62) orthorhombic unit cell;  $s$ ,  $m$  and  $l$  denote short, medium and long Mn-O bonds of  $MnO_6$  octahedra;  $d_O$  is the distance between oxygens O(1) and O(2) shown in Fig. 1(b) of the main text; IPA and OPA are the Mn-O-Mn bond angles within the  $ab$  planes and along the  $c$  direction, respectively. All the lengths are in Å and all the angles are in degrees.

	GdMnO <sub>3</sub>		TbMnO <sub>3</sub>		HoMnO <sub>3</sub>		ErMnO <sub>3</sub>		YbMnO <sub>3</sub>		LuMnO <sub>3</sub>	
	Exp. <sup>5</sup>	PS	Exp. <sup>6</sup>	PS	Exp. <sup>7</sup>	PS	Exp. <sup>8</sup>	PS	Exp. <sup>9</sup>	PS	Exp. <sup>10</sup>	PS
$a$	5.318	5.261	5.293	5.240	5.257	5.203	5.227	5.186	5.216	5.154	5.190	5.137
$b$	5.866	5.807	5.838	5.797	5.835	5.771	5.792	5.759	5.799	5.725	5.785	5.706
$c$	7.431	7.367	7.403	7.342	7.361	7.301	7.327	7.282	7.299	7.253	7.282	7.241
$s$	1.911	1.916	1.905	1.915	1.904	1.912	1.910	1.911	1.879	1.908	1.899	1.907
$m$	1.944	1.934	1.940	1.934	1.944	1.936	1.938	1.936	1.940	1.940	1.942	1.942
$l$	2.228	2.182	2.221	2.180	2.223	2.173	2.194	2.170	2.262	2.160	2.206	2.155
$l_{O-O}$	3.097	3.071	3.057	3.047	3.020	3.007	2.993	2.990	2.907	2.959	2.967	2.945
IPA	145.98	145.80	145.36	145.08	144.08	143.85	143.66	143.32	140.51	142.32	142.26	141.81
OPA	145.68	145.38	145.04	143.19	142.46	141.08	141.91	140.15	140.27	138.40	139.30	137.51

Table III. Experimentally measured and theoretically optimized lattice parameters of films of o- $RMnO_3$ .  $a$ ,  $b$  and  $c$  are the lattice constants of  $Pbnm$  (#62) orthorhombic unit cell;  $s$ ,  $m$  and  $l$  denote short, medium and long bonds of  $MnO_6$  octahedra;  $d_O$  is a distance between oxygens O(1) and O(2) shown in Fig. 1(b) of the main text; IPA and OPA are the Mn-O-Mn bond angles within the  $ab$  planes and along the  $c$  direction, respectively. All the lengths are in Å and all the angles are in degrees.

	GdMnO <sub>3</sub>		TbMnO <sub>3</sub>		HoMnO <sub>3</sub>		ErMnO <sub>3</sub>		YbMnO <sub>3</sub>		LuMnO <sub>3</sub>			
	10 nm		14 nm		120 nm		30 nm		400 nm		26 nm		104 nm	
	Exp. <sup>4</sup>	PS	Exp. <sup>3</sup>	PS	Exp.	PS	Exp.	PS	Exp.	PS	Exp.	PS	Exp.	PS
$a$	5.183	5.128	5.182	5.130	5.275	5.220	5.174	5.132	5.224	5.161	5.220	5.167	5.220	5.167
$b$	5.976	5.935	5.936	5.893	5.780	5.736	5.828	5.780	5.771	5.699	5.734	5.595	5.753	5.651
$c$	7.372	7.309	7.367	7.307	7.429	7.368	7.360	7.315	7.361	7.315	7.492	7.450	7.379	7.338
$s$	-	1.909	-	1.909	-	1.914	-	1.908	-	1.909	-	1.910	-	1.909
$m$	-	1.915	-	1.921	-	1.951	-	1.940	-	1.953	-	1.990	-	1.965
$l$	-	2.204	-	2.195	-	2.164	-	2.167	-	2.153	-	2.120	-	2.141
$l_{O-O}$	-	3.000	-	2.990	-	3.025	-	2.970	-	2.973	-	3.008	-	2.978
IPA	-	144.81	-	144.30	-	143.89	-	142.95	-	142.27	-	141.75	-	141.85
OPA	-	145.09	-	143.88	-	141.50	-	140.93	-	138.85	-	138.72	-	138.02

## II. EXCHANGE INTERACTIONS AND ANISOTROPIES

In Tables IV and V we summarize the Heisenberg ( $J_c$ ,  $J_{ab}$ ,  $J_a$ ,  $J_{diag}$ ,  $J_b$  and  $J_{3nn}$ ), biquadratic ( $B_c$  and  $B_{ab}$ ) and four-spin ring ( $K_c$  and  $K_{ab}$ ) exchange interactions as well as the Dzyaloshinskii-Moriya interaction (DMI,  $\gamma_{ab}$  and  $\alpha_c$ ) and single ion anisotropy ( $A$ ) parameters calculated using DFT for bulk samples and films of o- $RMnO_3$ , respectively.

In Fig. 1 we present the calculated couplings  $J_a$ ,  $J_{diag}$ ,  $B_c$ ,  $K_{ab}$ ,  $\gamma_{ab}$  and  $\alpha_c$  and anisotropies A versus the radius of the  $R$  cations for the bulk and film geometries.

\* natalya.fedorova@mat.ethz.ch

† nicola.spaldin@mat.ethz.ch

<sup>1</sup> Y. W. Windsor, M. Ramakrishnan, L. Rettig, A. Alberca, E. M. Bothschafter, U. Staub, K. Shimamoto, Y. Hu, T. Lippert, and C. W. Schneider, Phys. Rev. B **91**, 235144 (2015).

<sup>2</sup> H. Wadati, J. Okamoto, M. Garganourakis, V. Scagnoli, U. Staub, Y. Yamasaki, H. Nakao, Y. Murakami, M. Mochizuki, M. Nakamura, et al., Phys. Rev. Lett. **108**, 047203 (2012).

Table IV. Heisenberg ( $J_c$ ,  $J_{ab}$ ,  $J_a$ ,  $J_{diag}$ ,  $J_b$ ,  $J_{3nn}$ ), four-spin ring ( $K_{ab}$  and  $K_c$ ) and biquadratic ( $B_{ab}$  and  $B_c$ ) exchanges, components of DM vectors ( $\gamma_{ab}$  and  $\alpha_c$ ) and single-ion anisotropies ( $A$ ) (in meV) calculated using DFT for bulk o-RMnO<sub>3</sub>.

$R$	$J_c$	$J_{ab}$	$J_a$	$J_{diag}$	$J_b$	$J_{3nn}$	$K_{ab}$	$K_c$	$B_{ab}$	$B_c$	$\gamma_{ab}$	$\alpha_c$	$A$
Gd	4.34	-7.04	-0.99	0.75	0.67	2.82	0.24	0.91	-2.25	-0.44	-0.57	-0.50	-0.47
Tb	4.35	-6.03	-0.96	0.73	0.76	2.75	0.23	0.90	-2.20	-0.43	-0.57	-0.47	-0.48
Ho	4.33	-4.44	-0.95	0.72	0.95	2.69	0.21	0.92	-1.75	-0.42	-0.57	-0.42	-0.48
Er	4.20	-3.81	-0.99	0.69	0.95	2.68	0.28	0.90	-2.25	-0.45	-0.58	-0.40	-0.49
Yb	4.03	-2.73	-0.96	0.68	1.07	2.68	0.28	0.94	-2.22	-1.13	-0.58	-0.37	-0.48
Lu	3.96	-2.20	-0.94	0.68	1.13	2.70	0.28	0.96	-2.29	-0.88	-0.61	-0.35	-0.47

Table V. Heisenberg ( $J_c$ ,  $J_{ab}$ ,  $J_a$ ,  $J_{diag}$ ,  $J_b$ ,  $J_{3nn}$ ), four-spin ring ( $K_{ab}$  and  $K_c$ ) and biquadratic ( $B_{ab}$  and  $B_c$ ) exchanges, components of DM vectors ( $\gamma_{ab}$  and  $\alpha_c$ ) and single-ion anisotropies ( $A$ ) (in meV) calculated using DFT for the films of o-RMnO<sub>3</sub>. Lu<sup>(1)</sup> correspond to 104 nm film, Lu<sup>(2)</sup> - 26 nm film, Lu<sup>(3)</sup> - inv104 case, Lu<sup>(4)</sup> - inv26 case.

$R$	$J_c$	$J_{ab}$	$J_a$	$J_{diag}$	$J_b$	$J_{3nn}$	$K_{ab}$	$K_c$	$B_{ab}$	$B_c$	$\gamma_{ab}$	$\alpha_c$	$A$
Gd	7.80	-1.27	-0.82	0.70	1.02	2.22	0.20	0.71	-1.82	0.43	-0.51	-0.42	-0.52
Tb	4.35	-6.03	-0.96	0.73	0.76	2.75	0.23	0.90	-2.20	-0.43	-0.57	-0.47	-0.48
Ho	2.60	-6.51	-1.00	0.72	0.79	2.90	0.21	0.99	-2.33	-1.21	-0.63	-0.51	-0.44
Er	4.18	-2.79	-0.97	0.69	1.02	2.61	0.27	0.90	-2.23	-0.62	-0.60	-0.44	-0.47
Yb	2.88	-4.29	-1.02	0.69	0.95	2.85	0.29	1.01	-2.39	-0.54	-0.63	-0.45	-0.44
Lu <sup>(1)</sup>	1.98	-5.48	-1.10	0.68	0.87	3.04	0.33	1.08	-2.65	-2.16	-0.70	-0.48	-0.41
Lu <sup>(2)</sup>	0.14	-8.68	-1.16	0.78	0.85	3.48	0.12	1.32	-2.52	-4.71	-0.96	-0.69	-0.33
Lu <sup>(3)</sup>	5.85	1.23	-0.82	0.71	1.37	2.31	0.25	0.83	-1.74	0.31	-0.52	-0.23	-0.52
Lu <sup>(4)</sup>	6.67	3.22	-0.78	0.65	2.16	1.46	0.77	0.67	-2.65	0.07	-0.44	-0.09	-0.57

<sup>3</sup> K. Shimamoto, S. Mukherjee, S. Manz, J. S. White, M. Trassin, M. Kenzelmann, L. Chapon, T. Lippert, M. Fiebig, C. W. Schneider, et al., Scientific Reports **7**, 44753 (2017).

<sup>4</sup> K. Shimamoto, S. Mukherjee, N. S. Bingham, A. K. Suszka, T. Lippert, C. Niedermayer, and C. W. Schneider, Phys. Rev. B **95**, 184105 (2017).

<sup>5</sup> T. Mori, N. Kamegashira, K. Aoki, T. Shishido, and T. Fukuda, Materials Lett. **54**, 238 (2002), ISSN 0167-577X.

<sup>6</sup> J. A. Alonso, M. J. Martínez-Lope, M. T. Casáis, and M. T. Fernández-Díaz, Inorg. Chem. **39**, 917 (2000).

<sup>7</sup> A. Muñoz, M. T. Casáis, J. A. Alonso, M. J. Martínez-Lope, J. L. Martínez, and M. T. Fernández-Díaz, Inorg. Chem. **40**, 1020 (2001).

<sup>8</sup> F. Ye, B. Lorenz, Q. Huang, Y. Q. Wang, Y. Y. Sun, C. W. Chu, J. A. Fernandez-Baca, P. Dai, and H. A. Mook, Physical Review B **76**, 060402 (2007).

<sup>9</sup> M. Tachibana, T. Shimoyama, H. Kawaji, T. Atake, and E. Takayama-Muromachi, Phys. Rev. B **75**, 144425 (2007).

<sup>10</sup> H. Okamoto, N. Imamura, B. Hauback, M. Karppinen, H. Yamauchi, and H. Fjellvåg, Solid State Comm. **146**, 152 (2008).

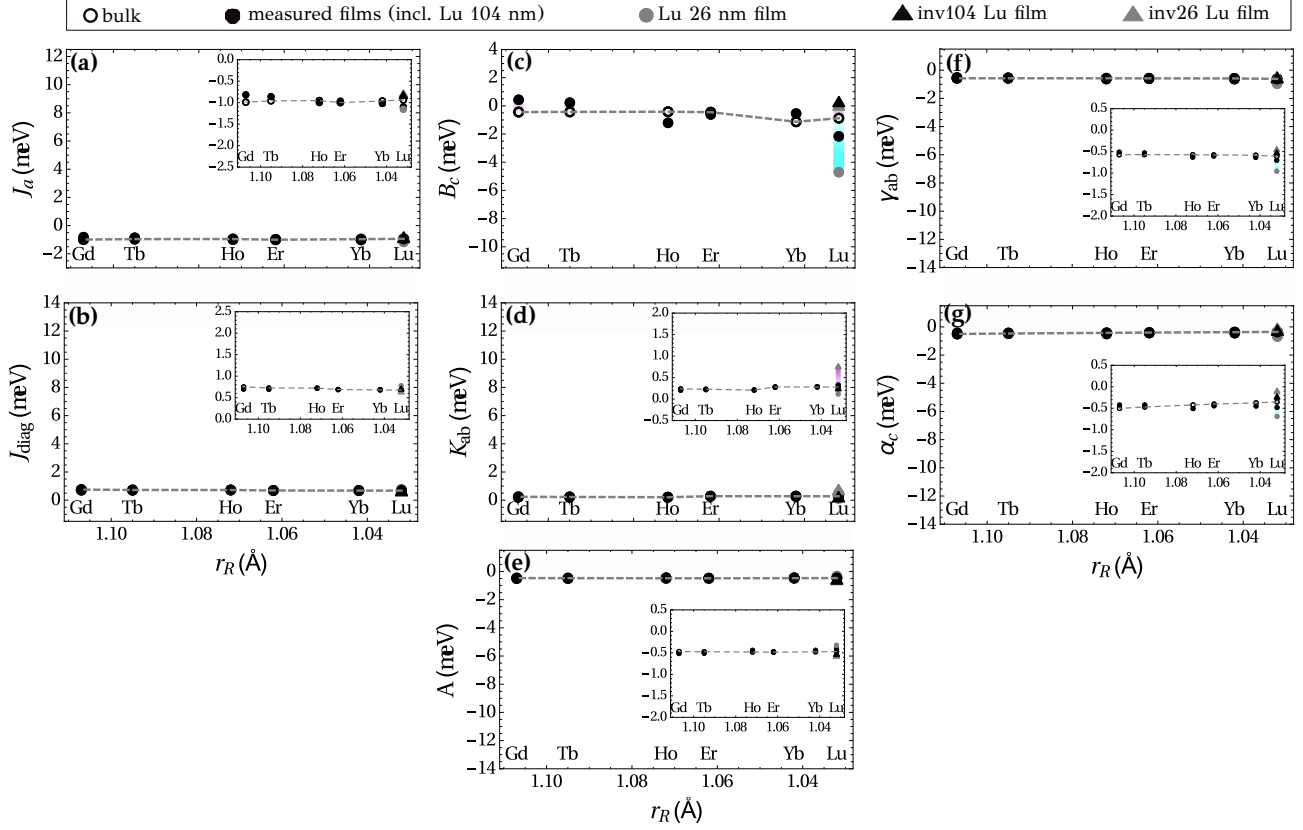


Figure 1. Calculated exchange couplings, components of DM vectors and anisotropy constants versus the radius of the  $R$  cation: (a) and (b) show the Heisenberg exchanges  $J_a$  and  $J_{diag}$ , respectively; (c) - biquadratic interplane exchanges  $B_c$ ; (d) - four-spin ring couplings  $K_{ab}$ ; (e) - SIA  $A$ ; (f) and (g) - the components of DM vectors  $\gamma_{ab}$  and  $\alpha_c$ , respectively. Bulk samples are shown by the empty circles, experimentally measured strained films - by the filled circles. In most cases filled and empty circles are on top of each other. For  $\text{LuMnO}_3$  the triangles denote the films which are compressively strained in the  $ac$  plane by the same amount (but opposite direction) as experimentally measured tensile strained films.  $\text{LuMnO}_3$  26 nm film and corresponding inverse case are highlighted in gray, 104 nm and inv104 case - in black. Compressive strain within the  $ac$  planes of the o- $RM\text{nO}_3$  films shown by the violet color, tensile strain - by the blue color. Dashed line connecting the data points for the bulk o- $RM\text{nO}_3$  is used to guide eye.